Spontaneous correction of angular fracture deformity in the rat

Jian Li[1], Mahmood Ahmed[1], Eva Samnegård[2], Tashfeen Ahmad[1], Andre Stark[1] and Andris Kreicbergs[1]

[1]Section of Orthopedics, Department of Surgical Sciences, Karolinska Institute, Stockholm, [2]Center for Surgical Sciences, Karolinska Institute at Huddinge University Hospital, Stockholm, Sweden
Correspondence JL: jianli@ki.se
Submitted 04-02-03. Accepted 04-09-21

Background **The different parts of long bone are known to participate in the spontaneous correction of fracture deformity. However, the relative contribution of growth plate, epiphysis and diaphysis of bone during the correction process is not clear.**

Animals and methods **We used a rat model of tibial fracture fixed with a semi-rigid intramedullary pin in anterior angulation, and evaluated the magnitude, temporal course and pertinent sites of spontaneous deformity correction by means of radiography and bone mineral uptake.**

Results **Over a 12-week period, the mean angular deformity was corrected from 27° to 11°. The major portion of the correction (14° of 16°) occurred within 3 weeks, concomitantly with fracture healing. The angle of the proximal growth plate changed 8° over the study period. The first 3 weeks were characterized by intense bone formation on the concave side of the fracture. From weeks 3–8, signs of resorption predominated on the corresponding convex side. On the concave side, the front of new bone formation in the proximal diaphysis moved in the opposite direction to that at the fracture level, so that both sites contributed to deformity correction.**

Interpretation **We found that different sites of a diaphyseal bone fractured in angulation respond quite differently, but still in an orchestrated way to promote correction by modeling. Notably, most of the spontaneous correction occurred during the reparative phase, the major contributor being the diaphysis, not the growth plate. Compared to other reports on angulated fracture using rigid fixation and limb immobilization, our data suggest that semi-rigid fixation and early weight bearing is more efficient in enhancing not only healing, but also deformity correction.** ■

The mechanisms regulating local bone turnover, often occurring as an uncoupled process between bone formation and resorption, are poorly understood. These mechanisms presumably play an important role not only in pathological conditions characterized by osteolysis or sclerosis, but also in continuous bone remodeling and spontaneous correction of fracture deformity as often seen in pediatric orthopedics. A variety of factors have been suggested to regulate local bone turnover, such as cytokines (Siggelkow et al. 2003), growth factors (Silha et al. 2003), neuronal mediators (Li et al. 2001, Irie et al. 2002) and systemic hormones (Abe et al. 2003). Much emphasis has been placed on the role of mechanical forces in regulating bone architecture in accordance with Wolff's law, later modified by Jee (1989) and Frost (1990, 2001). An illustrative clinical example of the adaptive capacity of bone is seen in pediatric patients with angulated fracture. It is not known how mechanical forces are monitored and conveyed to elicit adaptive responses. Also, the magnitude, temporal course and pertinent sites of spontaneous correction of fracture deformity by modeling have not been clarified satisfactorily. It may be that semi-rigid fixation combined with early axial weight bearing not only enhances healing, but also correction of long bone deformity.

Recently, we reported a fracture deformity model in the rat which elicits site-specific differences in bone formation and resorption (Li et al. 2004). By angulating a mid-shaft tibial fracture fixed with an intramedullary pin permitting early weight bearing, intense bone formation on the concave side and a

DOI 10.1080/17453670510041358

predominance of bone resorption on the convex side occurred. These site-specific differences in response can be exploited to assess—both morphologically and quantitatively—the difference in expression of relevant markers of local bone turnover in one and the same bone. In the present study, our aim was to analyze the temporal course and magnitude of spontaneous correction of fracture deformity, and the relative contribution of the growth plate and the diaphysis in this process.

Animals and methods

Animals, housing and grouping

30 male Sprague-Dawley rats, mean weight 200 (180–220) g, were housed 3 per cage with free access to standard rat chow and tap water in the animal room of Karolinska Hospital. The temperature was controlled (21°C), with a 12 h light/dark cycle. 15 rats were assigned to each of two fracture groups, i.e., one with anterior angulation and another with straight alignment. In each group, 12 rats were used for radiographic assessment and 3 were used for bone mineralization analysis. All animal experiments were performed with approval from the Animal Research Ethics Committee, Stockholm North, Sweden.

Surgery

Under anesthesia with fentanyl-fluanisone (Hypnorm 0.5 mL/kg body weight, Janssen Pharmaceutica, Beerse, Belgium), the mid-diaphysis of the right tibia in both groups was fractured manually by three-point bending, and fixed internally with a semi-rigid pin (17-gauge cannula needle) as described previously (Li et al. 2001, 2004). Briefly, the intramedullary pin was inserted through a proximal hole at the tibial tuberosity without prior intramedullary reaming. In half of the rats, the fracture was fixed in anterior angulation (approximately 40°), including the normal anterior curve of the tibia, i.e., 13°. In the remaining half, which served as controls, the fracture was fixed in normal straight alignment, i.e. in 13° anterior curve. No measures were taken to restrict weight bearing.

Radiography

Repeated radiographic investigations over 12 weeks, including lateral and AP views to assess fracture alignment and adequacy of internal fixation, were done under Hypnorm anesthesia immediately after surgery and then at weeks 3, 5, 8, and 12 postoperatively. A dental radiograph machine (Heliodent DS, Siemens AG, Bensheim, Germany) with 1.25 sec. exposure time on 56 × 76 mm X-ray films (Ektaspeed Plus, Eastman Kodak Company, Rochester, NY) was used. Radiography was done on a previously described special platform (Li et al. 2004), which results in a 33% magnification of the original image. The films were then developed and scanned (HP ScanJet II) and the images saved on a computer.

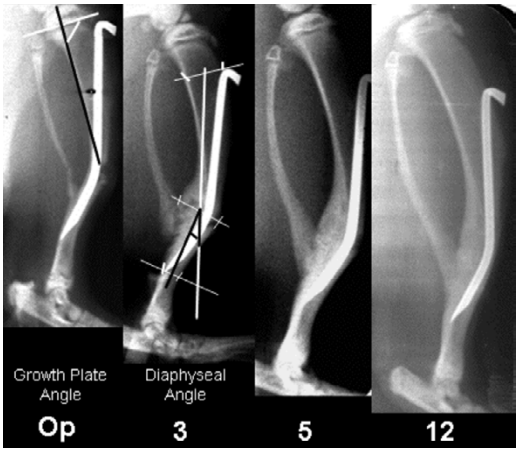

Figure 1. Serial radiography showing the healing and correction process over 12 weeks. This includes reference points and lines for measurement of the angle of the proximal growth plate and diaphysis, as well as the diaphyseal length. Op = operation.

In order to measure the diaphyseal angle, the angle of the proximal growth plate and the length of tibia several reference points were defined. The measurement of diaphyseal angle was based on three reference points, i.e., the proximal and distal tip, and also the apex of the angulated nail. The position of the proximal growth plate was defined by the angle between a line along the proximal growth plate and another along the posterior cortical border of the proximal metaphysis (Figure 1). The thicknesses of the bone anterior and posterior to the nail were measured in mm at the level of the apex of the angulated pin. The length of the tibia was measured in order to assess growth of the proximal and distal segments, respectively. Thus, the tibial length was defined as the sum of two dis-

tances: that between the upper end of the proximal epiphysis to the tibio-fibular synostosis and that between the synostosis and the lower end of the distal epiphysis. All the measurements were done manually on 3× magnified printout pictures.

Bone mineralization

3 rats from each fracture group were injected subcutaneously with Calcein (8 mg/kg) and Alizarin Red (30 mg/kg) (both dyes from Sigma, Steinheim, Germany) on alternate weeks until week 14 (Li et al. 2004). 1 week after the last injection, the rats were killed by intraperitoneal pentobarbital sodium overdose and both tibias were dissected and fixed in 70% ethanol for 3 days. The diaphysis was cut transversely into two parts through the apex of the fracture site, and the nail was pulled out. A 1.5-cm segment proximal to the transverse cut and another 1-cm segment distal to the transverse cut were dissected and kept in Villanueva block stain and then embedded in methyl methacrylate (Baron et al. 1983, Villanueva and Lundin 1989). 5 sagittal sections were taken from the proximal segment and 5 cross-sections from the distal segment were taken at 70 µm thickness with a Leica 1600 saw/microtome (Nussloch, Germany). The sections were fixed on slides with Pertex (Histolab Products AB, Gothenburg, Sweden), mounted with coverslips and examined under an epifluorescence microscope (Eclipse E800; Nikon, Yokohama, Japan) connected to a Nikon DXM 1200 video camera for photography. Using a 4 × objective, pictures were taken from each section and assembled on the computer to obtain a montage. Calcein-labeled areas (green) reflect newly formed woven and lamellar bone. Alizarin Red-labeled areas separate the green bands, permitting analysis of the temporal course of bone mineralization.

Statistics

The mean values (SD) were calculated. Analysis of variance was used for comparisons between study periods. A p-value < 0.05 was considered to be a significant difference (two-tailed).

Results

All rats resumed weight bearing within a few hours of fracture, but limped for 4–7 days. No infection or secondary deformity was seen. 1 rat in each group died due to anesthesia at radiography.

Radiography

Postoperatively, initial deformity radiographs of the tibia showed a mean deformity of fracture of 27° (5°) in the anterior angulation group and 2° (0.5°) deformity in the straight alignment group. The angle of the proximal growth plate of contralateral un-fractured tibia remained unchanged at 92° (2°) in both fracture groups.

Healing. In the anterior angulation group, bridging callus—most evident on the concave side—was seen at 3 weeks after fracture. Complete healing took 5 weeks. While the callus size on the concave side remained essentially the same as at 3 weeks until the end of the experiment, it decreased continuously on the convex side until the apex of the angulated nail perforated the anterior cortex in some animals. An increasingly thicker rim of high density was seen along the whole border of the posterior cortex of the tibia (Figure 1).

In the straight alignment fracture, healing was observed 3 weeks after fracture. Compared to the anterior angulation group, a smaller callus was found and it was equally distributed around the fracture site. After 3 weeks, the callus size decreased equally on the concave and convex sides. The thin rim of bone density along the posterior cortex remained unchanged over time.

Bone thickness. The thickness of bone at fracture level in the angulated group increased significantly on both the concave and convex sides during the first 3 weeks, i.e. from 2.1 (0.6) mm to 9.5 (2.2) mm and from 3.6 (0.9) mm to 4.3 (2.2) mm. Subsequently, however, bone thickness on the convex side decreased continuously to 2.6 (2.2) mm ($p = 0.02$) at the end of experiment. In the straight alignment fracture group, bone thickness on the posterior and anterior sides increased symmetrically during the first 3 weeks, i.e. from 2.5 (0.6) mm to 7.2 (2.3) mm and from 3.5 (0.8) mm to 7.4 (2.7) mm, respectively, after which it became continuously reduced in a symmetrical manner.

Correction of deformity. In the angulated group, the fracture angle at 3 weeks had corrected by 14°, i.e. from 27° to 13°. A further 2.5° correction was

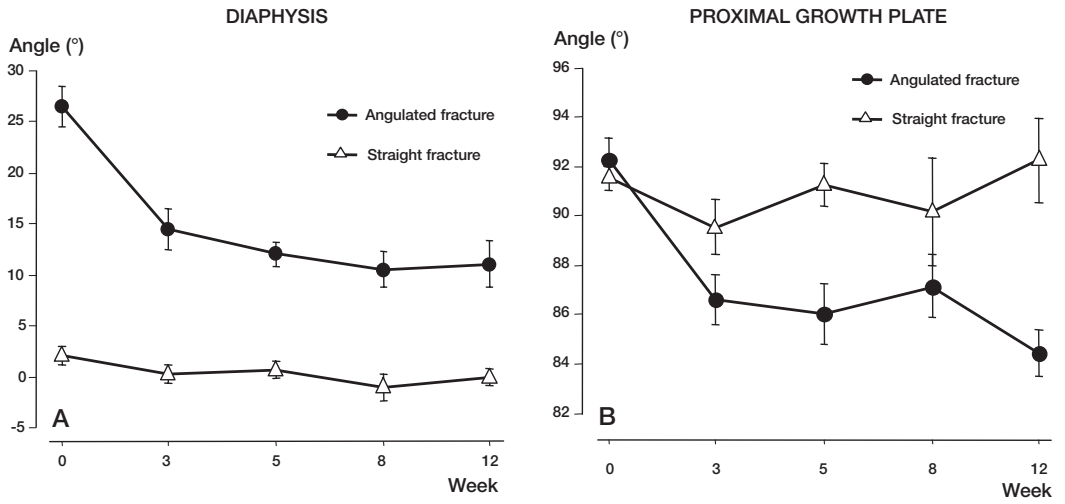

Figure 2. Changes in the angle of the diaphysis (A) and proximal growth plate (B) over 12 weeks in both the angulated and straight alignment group, presented as mean (SEM). Note that most of the deformity correction in the angulated group occurred within the first 3 weeks following fracture.

achieved before the end of the experiment at 12 weeks. The angle of the proximal growth plate side changed by 6° (2°), i.e. from 92° to 86°, during the first 3 weeks after fracture, and an additional 2° subsequently (Figure 2). On the contra-lateral unfractured side, no change in the angle of the proximal growth plate was observed. In the straight alignment group, the initial 2° fracture angle was almost completely corrected within 3 weeks following fracture. The angle of the proximal growth plate remained unchanged in both the fractured and contra-lateral unfractured tibia over the 12 weeks of the experiment.

Length of tibia. Measurement of the proximal and distal tibia showed that the bone grew from 42 (0.6) mm to 52 (1.6) mm in the angulated group and from 42 (1.2) mm to 53 (1.0) mm in the straight alignment group over the 12-week study period. When comparing the increase in length of the proximal and distal fractured tibia, it appeared that almost all the increase in length had taken place in the proximal part in both experimental groups (Figure 3). We found no statistical significance in the changes in length between groups for both the proximal and distal tibia.

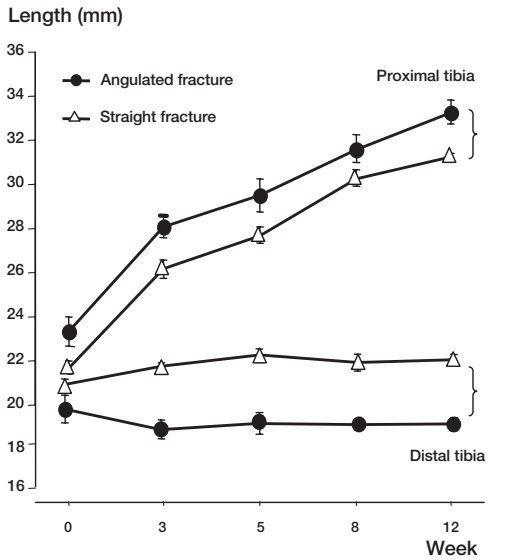

Figure 3. Changes in length of the proximal and distal fractured tibia in the angulated and straight alignment group over 12 weeks, presented as mean (SEM). This shows a clear difference in growth between the proximal and distal fragments, but not between the angulated and straight alignment groups.

Mineralization

Two types of tissue sections (cross-sections and longitudinal sections) were analyzed (Figure 4A). In the longitudinal sections (Figure 4B), we compared the anterior and posterior sides at two levels: at fracture level and higher up in the proximal diaphysis. In the cross-sections (Figure 4C-D), comparison of mineral uptake was done between

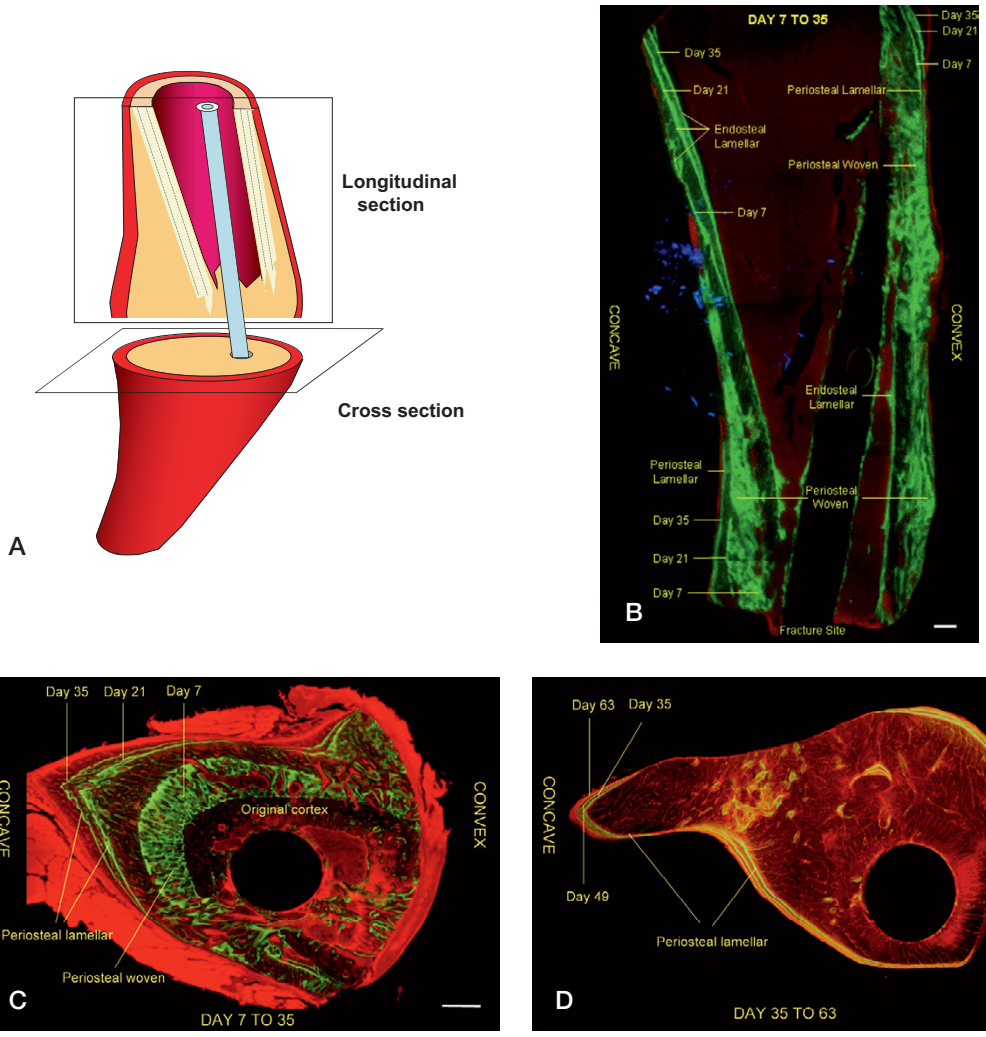

Figure 4. Schematic illustration showing types of tissue sections (A) taken for analysis of bone dye uptake and fluorescence photomicrographs of mineralization over time. In the longitudinal section (B: proximal diaphysis) and cross-sections (C and D: fracture level) in the angulated group, the lines denote origin (endosteal vs. periosteal) and type (woven vs. lamellar) of new bone formation. Green staining represents the uptake of calcein and red staining the uptake of Alazerin. Day refers to the day of injection of calcein. Bar represents 0.5 mm.

the anterior (convex), posterior (concave) and lateral sides at the level of the fracture.

Anterior angulation group. In the cross-sections from the fracture site at day 21, substantial new bone formation was seen on the concave side, less on the medial and lateral sides and least on the convex side (Figure 4C). As opposed to the posterior side, the cortex of the anterior side gradually became thinner up to day 84, reflecting periosteal bone resorption (Figure 4D). In the cross-section, this resulted in a pear-shaped repair tissue with the medullary canal located eccentrically near the convex aspect (Figure 4C-D). The new bone formed was exclusively of woven type from day 7 up to day 21, after which it gradually switched to lamellar type (Figure 4C). From day 35 to day 84, only lamellar bone formed on the medial, lateral and concave sides, and virtually no signs of new bone formation could be seen on the convex side (Figure 4D).

The longitudinal sections provided an overview of the magnitude, temporal course, type and sites of new bone formation and (indirectly) also resorption (Figure 4B). From day 7 to day 35, both woven and lamellar bone formations were seen

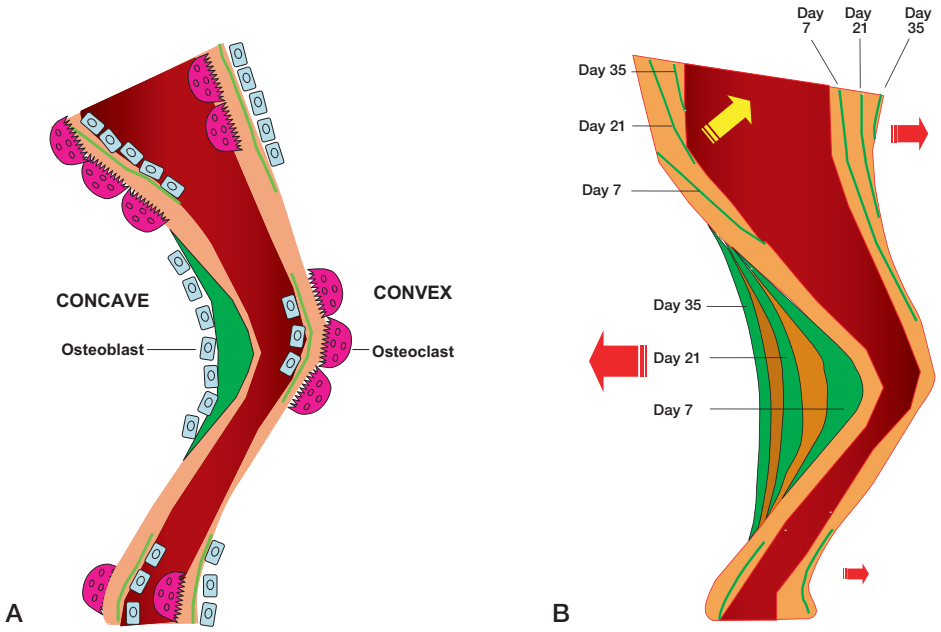

Figure 5. Schematic illustration of the predominant bone formative and resorptive cell activity in different parts of the diaphysis (A) and the resulting diaphyseal drift (B) over time. Green color depicts the site and amount of new bone formation. Day refers to the day of injection of calcein.

on the posterior aspect (concave side) at fracture level, where a large amount of periosteal woven bone was formed, and later also periosteal lamellar bone. However, higher up in the proximal diaphysis only endosteal lamellar bone formation was seen, which proceeded anteriorly from the posterior cortex, i.e. in the opposite direction to the periosteal lamellar bone formation at the fracture level. Notably, the mineralization front of endosteal lamellar bone ran obliquely across the posterior cortex, as shown in Figure 4B and as illustrated in Figure 5A-B. It also appeared that the greater the distance from the fracture proximally, the greater was the degree of subperiosteal resorption and endosteal formation in the posterior cortex. On the anterior aspect (convex side) of the diaphysis at the fracture level, a single layer of lamellar bone was seen endosteally, while periosteally only woven bone was observed. Proximally, no endosteal lamellar bone formation was seen, however, but some periosteal woven bone formation was observed and, later on, periosteal lamellar bone formation also.

From day 35 to day 84, the longitudinal sections exclusively showed lamellar bone formation, both at the fracture level and higher up proximally. At the fracture level on the posterior aspect, bone formation proceeded posteriorly from the periosteum. On the anterior aspect of the fracture, almost no new bone formation was observed from day 35 onwards. In the proximal diaphysis on the posterior aspect, lamellar bone formation proceeded from the endosteum anteriorly, concomitantly with periosteal bone resorption. On the anterior aspect, periosteal lamellar bone formation proceeded anteriorly.

Straight alignment group. In the controls, the pattern of new bone formation differed clearly from that seen in the angulated fractures. In the cross-sections at the fracture level, new bone of predominantly woven type was equally distributed around the diaphysis between days 7 and 35. From day 35 onwards, only lamellar bone was formed. In the longitudinal sections, mainly periosteal woven bone was seen up to week 5 along the whole anterior aspect, although it was more evident at fracture level than proximally. On the posterior aspect, only endosteal lamellar bone formation was seen proceeding anteriorly from the posterior cortex, both at the fracture level and higher up proximally.

Discussion

Our study shows that most of the spontaneous correction of an angular fracture deformity occurs during early healing. In contrast to previous reports (Wolff 1892, Karaharju et al. 1976 Abraham 1989, Wallace and Hoffman 1992, Murray et al. 1996), the contribution of the diaphysis in correcting the deformity is greater than that of the growth plate. The diaphyseal correction is mainly achieved through a mechanism by which the front of new bone formation proceeds in opposite directions at fracture level and higher up in the proximal diaphysis. It appears that semi-rigid fixation permitting micromotion at the fracture site and early weight bearing not only enhance healing, but they also improve deformity correction.

In our study, 60% of the initial tibial angulation was corrected over the study period, i.e. from 27° to 11°, which is in agreement with the observations of Kwon and Moon (1980), who demonstrated a 17° correction of rat tibia that was left without fixation. The fact that the spontaneous correction in these two studies failed to restore the deformity completely seems to reflect the fact that there is an inherent limitation in the capacity to remodel. In our study, part of the incomplete correction may also be attributed to the intramedullary pin resisting the spontaneous correction. Nonetheless, the corrective force surmounted this resistance, as reflected by the cortical penetration of the pin in several animals. A prolonged study period would probably not have disclosed any further correction, as only 2.5° was gained between 5 and 12 weeks.

In previous reports on angular fracture deformity (Karaharju et al. 1976, Abraham 1989, Wallace et al. 1992, Murray et al. 1996), the growth plate has been claimed to be the major contributor to spontaneous correction. As much as 75% of the total correction has been attributed to this site in a growing long bone, as compared to a maximum of 45% in the diaphysis (Abraham 1989). These observations differ decisively from our findings. Thus, the position of the proximal growth plate of angular tibia changed by only 8°, while the diaphyseal angle changed by 16° over the study period. In a study on young rabbits, Murray et al. (1996) found that the angle of the growth plate had changed by 12° and that of the diaphysis by only 4°. These results, which conflict with ours on the relative contribution of the growth plate and diaphysis in correcting the deformity, should mainly be attributed to the difference in surgical fixation. With rigid fixation, greater demand for adjustment is put on the growth plate. While Murray et al. used rigid fixation of the angulated tibia, we used a semi-rigid fixation, and this permitted greater mechanical load and micromotion at the fracture site, which enhances healing through indirect osteogenesis and callus formation. Admittedly, one other explanation for the discrepancy between the results may be the higher osteogenic capacity of rat compared to rabbit. Furthermore, our measurements differed from those in earlier studies. Instead of defining one proximal and one distal reference point for the whole tibia, we measured the proximal and distal fragments of the tibia separately, in order to avoid some of the problems associated with length measurements of a curved bone. This approach also minimizes the error in measuring the angles of interest.

Surprisingly, in our study we found that most of the deformity correction occurred concomitantly with the fracture repair phase. The prevailing idea that the main correction of fracture deformity takes place after healing seems to be unfounded. Given continuous mechanical load, it appears that the early healing phase, characterized by high bone turnover, also strongly promotes correction of fracture deformity. By avoiding rigid fixation and permitting early weight bearing, this high bone turnover during the early healing phase can be exploited to obtain maximum spontaneous correction of the deformity. As for the mechanisms underlying spontaneous correction of fracture deformity, they are basically unknown. Although mechanical load may be assumed to play an important role, the question of how this modality is registered and conveyed to elicit adaptive responses remains unsolved. Direct effects of mechanical load on the cytoskeleton and also neuronal regulation of bone cells via the receptors have been suggested (Korcok et al. 2004, Mason 2004). Apart from these cellular mechanisms, it also remains unknown how and where the correction occurs in a long bone. Our observations suggest that different sites of a fractured diaphyseal shaft respond quite differently in terms of bone formation and resorption (Figure 5A). At fracture level in the angulated

group, intense new bone formation was seen on the concave side, while resorption predominated on the convex side. In the straight alignment group, however, no such difference could be seen between the posterior and anterior sides. In the angulated group, the mineralization front on the concave side proceeded posteriorly at fracture level, but notably, in the opposite direction higher up in the proximal diaphysis—reflecting so-called drift (Figure 5B). In this area, virtually no periosteal woven bone could be seen, presumably because of high resorptive activity. Instead, lamellar bone formed endosteally. These features were almost reversed on the convex side of the proximal diaphysis, where woven as well as lamellar bone formed periosteally, thereby also contributing to the anterior drift of the whole proximal diaphysis.

The process in the proximal diaphysis, and in particular at the fracture site, may be seen as an expression of uncoupled bone formation-resorption mimicking the bone drift (so-called modeling) during normal growth (Jee 1989, Frost 1990, 2001). Although the distal diaphysis below the fracture site was not investigated in this study, it seems reasonable to assume that it underwent the same process. However, the length measurements over time showed that almost no growth occurred in the distal diaphysis as opposed to the proximal diaphysis. This implies that the contribution of the distal diaphysis to the correction by anterior drift was quite low compared to that of the proximal diaphysis. This strengthens the notion that skeletal growth is of decisive importance for correction of fracture deformity.

This study was supported by grants from the AO/ASIF Foundation, the Swedish Medical Research Council (13107) and the Swedish Institute.

No competing interests declared.

Abe E, Marians R C, Yu W, Wu X B, Ando T, Li Y, Iqbal J, Eldeiry L, Rajendren G, Blair H C, Davies T F, Zaidi M. TSH is a negative regulator of skeletal remodeling. Cell 2003; 115 (2): 151-62.

Abraham E. Remodeling potential of long bones following angular osteotomies. J Pediatr Orthop 1989; 9 (1): 37-43.

Baron R, Vignery A, Neff L, Silverglate A, Santa Maria A. Processing of undecalcified bone specimens for bone histomorphometry. In: Bone histomorphometry: Techniques and interpretation (ed Recker R R). CRC Press, Boca Raton, Florida, USA, 1983: 13-35.

Frost H M. Skeletal structural adaptations to mechanical usage (SATMU): 1. Redefining Wolff's law: the bone modeling problem. Anat Rec 1990; 226 (4): 403-13.

Frost H M. From Wolff's law to the Utah paradigm: insights about bone physiology and its clinical applications. Anat Rec 2001; 262 (4): 398-419.

Irie K, Hara-Irie F, Ozawa H, Yajima T. Calcitonin gene-related peptide (CGRP)-containing nerve fibers in bone tissue and their involvement in bone remodeling. Microsc Res Tech 2002; 58 (2): 85-90.

Jee W S S. The skeletal tissues. In: Cell and tissue biology. a textbook of histology (ed. Weiss L) Baltimore: Urban and Schwartzenberg, 1989: 211-59.

Karaharju E O, Ryoppy S A, Makinen R J. Remodelling by asymmetrical epiphysial growth. An experimental study in dogs. J Bone Joint Surg (Br) 1976; 58 (1): 122-6.

Korcok J, Raimundo L N, Ke H Z, Sims S M, Dixon S J. Extracellular nucleotides act through P2X7 receptors to activate NF-kappaB in osteoclasts. J Bone Miner Res 2004; 19 (4): 642-51.

Kwon D J, Moon M S. The influence of physeal injury upon growth correction of deformed rat tibia. Int Surg 1980; 65 (4): 341-5.

Li J, Ahmad T, Spetea M, Ahmed M, Kreicbergs A. Bone reinnervation after fracture: a study in the rat. J Bone Miner Res 2001; 16 (8): 1505-10.

Li J, Ahmad T, Bergström J, Samnegård E, Erlandsson-Harris H, Ahmed M, Kreicbergs A. Differential bone turnover in an angulated fracture model in the rat. Calcif Tissue Int 2004: Mar 25 [Epub ahead of print].

Mason D J. Glutamate signalling and its potential application to tissue engineering of bone. Eur Cell Mater 2004; 7: 12-25.

Murray D W, Wilson-MacDonald J, Morscher E, Rahn B A, Kaslin M. Bone growth and remodelling after fracture. J Bone Joint Surg (Br) 1996; 78 (1): 42-50.

Siggelkow H, Eidner T, Lehmann G, Viereck V, Raddatz D, Munzel U, Hein G, Hufner M. Cytokines, osteoprotegerin, and RANKL in vitro and histomorphometric indices of bone turnover in patients with different bone diseases. J Bone Miner Res 2003; 18 (3): 529-38.

Silha J V, Mishra S, Rosen C J, Beamer W G, Turner R T, Powell D R, Murphy L J. Perturbations in bone formation and resorption in insulin-like growth factor binding protein-3 transgenic mice. J Bone Miner Res 2003; 18 (10): 1834-41.

Villanueva A R, Lundin K D. A versatile new mineralized bone stain for simultaneous assessment of tetracycline and osteoid seams. Stain Technol 1989; 64: 129-38.

Wallace M E, Hoffman E B. Remodelling of angular deformity after femoral shaft fractures in children. J Bone Joint Surg (Br) 1992; 74 (5): 765-9.

Wolff J. Das Gesetz der Transformation der Knochen. Berlin: Verlag von August Hirschwald 1892.